

## Tetrahedral Site Ordering in Synthetic Gallium Albite: A $^{29}\text{Si}$ MAS NMR Study

BARBARA L. SHERRIFF,\*† MICHAEL E. FLEET, AND  
PETER C. BURNS†

*Department of Geology, University of Western Ontario, London,  
Ontario, N6A 5B7, Canada*

Received February 11, 1991; in revised form May 7, 1991

The ordering of Si in the tetrahedral sites of gallium albite ( $\text{NaGaSi}_3\text{O}_8$ ) has been studied by MAS NMR and Rietveld structure refinement of X-ray powder diffraction data. Low structural state (ordered) material was annealed at about  $800^\circ\text{C}$  under a load pressure of 1 kbar, and by Rietveld refinement has tetrahedral-site occupancies for Si of  $T_1O = 0.24(3)$ ,  $T_1m = 0.89(2)$ ,  $T_2O = 0.98(2)$ , and  $T_2m = 0.89(2)$ , respectively. Corresponding Si occupancies for high structural state (disordered) material are 0.71(2), 0.78(1), 0.76(2), and 0.74(2), respectively. The  $^{29}\text{Si}$  MAS NMR spectra of low gallium albite is equivalent to the three-peak spectrum of natural (Amelia) albite, with resonances at  $-89.6$ ,  $-96.4$ , and  $-104.2$  ppm but with relative peak areas of 0.79:1.0:0.77. The tetrahedral-site occupancies derived from the MAS NMR spectrum are in good agreement with those obtained by Rietveld refinement and, in particular, indicate that the  $-96.4$  ppm peak must correspond to Si in  $T_2O$ . This is the first independent assignment of the  $^{29}\text{Si}$  peak at  $-96$  ppm in the spectrum of ordered albite to the  $T_2O$  site. A peak at  $-96$  ppm is also resolved in the spectrum of high gallium albite. The systematic differences in peak position between the  $^{29}\text{Si}$  MAS NMR spectra of low gallium albite and those of Amelia albite cannot be explained simply by the direct replacement of Al by Ga, without a change in angle at the bridging oxygen atoms. © 1991 Academic Press, Inc.

### Introduction

The order-disorder transformation in albite ( $\text{NaAlSi}_3\text{O}_8$ ) has been studied by numerous earth and solid state scientists during the last three decades (for a brief review see Ref. (1)). Most studies have concerned the long-range Al/Si ordering in albite. The Al/Si distribution in high (disordered) albite involves an essentially random distribution

of Al over the four structurally distinct tetrahedral sites, designated  $T_1O$ ,  $T_1m$ ,  $T_2O$ , and  $T_2m$ . As ordering increases, Al is concentrated into the  $T_1O$  tetrahedral site and is conventionally thought to leave each of the other three sites in similar proportions. Experimental studies of the order-disorder transformation in albite have generally been plagued with the difficulty of demonstrating order-disorder equilibrium. However, recent studies of ordering in the albite structure indicate that the transformation is continuous over a range of temperatures (1, 2).

Gallium substituted albite (gallium albite,  $\text{NaGaSi}_3\text{O}_8$ ) was studied by Burns and

\* To whom correspondence should be addressed.

† Present address: Department of Geological Sciences, University of Manitoba, Winnipeg, Manitoba, R3T 2N2, Canada.

Fleet (1) following the work of Pentinghaus (3) and Pentinghaus and Bambauer (4) which indicated that the order-disorder transformation occurs very rapidly when gallium replaces the aluminum in albite. Gallium albite ( $\text{NaGaSi}_3\text{O}_8$ ) and albite ( $\text{NaAlSi}_3\text{O}_8$ ) are isostructural by infrared spectroscopy and X-ray powder diffraction (4), single crystal X-ray structure analysis (5-7), and Rietveld X-ray diffraction structure refinements (1). Burns and Fleet (1) were able to establish Ga/Si order-disorder equilibrium in synthetic gallium albite using dry annealing with load pressures of approximately 1 kbar. The order-disorder transformation in gallium albite occurs in the temperature range 890 to 970°C and is continuous and distinctly second order. Furthermore, as the X-ray scattering efficiencies of Ga and Si are markedly different, direct refinement of the tetrahedral-site occupancies was possible using the Rietveld structure refinement technique.

Plagioclase feldspars were among the first minerals to be studied with  $^{29}\text{Si}$  magic angle spinning nuclear magnetic resonance (MAS NMR) (8). The three peaks in the spectrum of Amelia albite, at -92.8, -96.7, and -104.2 ppm, were assigned to Si in the  $T_2m$ ,  $T_2O$ , and  $T_1m$  sites, respectively, by Higgins and Woessner (9) using the number of next nearest neighbor Al atoms and the mean Si-O bond distance as criteria. These peak allocations have been maintained by later authors using different criteria for correlating between the chemical shift and the local site environment (10-15).

This MAS NMR experiment was done to verify the accuracy of the Rietveld results and establish the feasibility of combining these two techniques in the study of cation order. The comparison of Rietveld and NMR derived site occupancies also gives further (independent) evidence that the three peaks in the spectra of Amelia albite are correctly assigned to the corresponding tetrahedral sites.

## Experimental

### *Synthesis of Gallium Albite*

Starting materials were prepared from purified  $\text{Ga}_2\text{O}_3$  and  $\text{SiO}_2$  and analytical grade  $\text{Na}_2\text{CO}_3$ , ground and mixed in an agate mortar. High structural state material was crystallized from a sodium tungstate melt using a mixture of 0.5 g nutrient to 4.5 g  $\text{Na}_2\text{WO}_4 \cdot 2\text{H}_2\text{O}$ . The flux mixture was contained in a platinum crucible with a tight fitting lid, soaked at 775°C for 72 hr, and cooled at 4°C/hr to 694°C for sample GbF12. Low structural state material was prepared by annealing GbF11 under a dry load pressure in a standard cold-seal hydrothermal vessel (1). To provide the quantity required for the MAS NMR study, large gold capsules were used and three separate batches were annealed for 44 hr each at 800 to 815°C and 0.7 to 1.0 kbar. Structural state was confirmed by X-ray powder diffraction. Sample GbF11 (low gallium albite) was annealed below the temperature range for order/disorder in  $\text{NaGaSi}_3\text{O}_8$  and is an equilibrium product (1), but sample GbF12 (high gallium albite) was crystallized from the flux mixture at room pressure and is metastable.

### *Nuclear Magnetic Resonance*

A magic angle spinning probe (16) with Delrin rotors was used with a Bruker AM-500 multinuclear Fourier transform NMR spectrometer equipped with a 11.74 Tesla superconducting magnet. The samples were spun at approximately 3000 Hz at an angle of 54.7° to the magnetic field.

$^{29}\text{Si}$  MAS NMR spectra were recorded at a frequency of 99.3 MHz with 8192 data points, a spectral width of 50,000 Hz, and 10- $\mu\text{sec}$  pulses. Various delays between pulses from 5 to 300 sec were tried and the relative peak areas for each delay compared despite the poor signal to noise of the spectra. As there was no apparent difference in peak intensity it was assumed that

all the nuclei were equally relaxed, and as a 60-sec delay gave the optimum signal-to-noise ratio in a reasonable time this was used to record the spectra. Peak positions were measured with reference to TMS (tetramethylsilane). Relative peak intensities were measured by cutting out the spectra and weighing individual peaks. This method has been found to give the same degree of accuracy, for separately resolved peaks, as fitting peaks to the spectra using a least-squares computer program and calculating the relative peak intensities (17).

<sup>29</sup>Si MAS NMR chemical shifts were calculated using the method of Sherriff and Grundy (18). Briefly, a series of equations relates the geometrical position, orientation, and valence of bonds between cations and terminal oxygens of the silicate tetrahedron to the chemical shift. The structure of ordered Amelia albite (19) was used as a basis for the calculation with Al being replaced by Ga and with the adjustment of Ga–O distances to 1.83 Å.

#### *X-Ray Diffraction and Rietveld Structure Refinements*

Powders for samples GBF11 and GBF11 and GBF12 were ground in an agate mortar for a minimum of 5 min, mixed with deionized water, and spread on zero-background quartz plates. The slurry mixtures were agitated until dry to minimize preferred orientation effects. Powder patterns were collected over the  $2\theta$  range  $10^\circ$ – $65^\circ$  with a Rigaku Geigerflex D/MAX-IIA automated X-ray diffraction system using monochromatized  $\text{CuK}\alpha$  radiation ( $\lambda = 1.54178 \text{ \AA}$ ). The powder pattern above this  $2\theta$  range is featureless with the present materials (1) and was excluded from the refinements. Step scans were digitized using a  $0.02^\circ$   $2\theta$  step interval and a 10-sec counting time per step (cf. (20, 1)). A step width considerably shorter than the optimal step width, which is approximately equal to the minimum full-width at half-maximum (FWHM) for rela-

tively simple patterns (21), was used to compensate for the complexity of the gallium albite powder patterns (1). The ensuing counting statistics result in some positive serial correlation of the residuals, and thus parameter standard deviations may be somewhat underestimated (21).

Rietveld structure refinements were completed using the program LHPM1 (22) as modified by Hill and Howard (21). Both structures were refined in the space group  $C1$ . The pseudo-Voigt peak profile function ( $v$ ,  $w$ ,  $\gamma_1$ ,  $\gamma_2$  refined) was used to model peak profiles. Unit-cell parameters derived from the X-ray powder patterns using the least-squares cell refinement program of Appleman and Evans (23) and the atomic coordinates of low albite ((24), Table 4-1) were used as parameter estimates for the first refinement runs. Backgrounds were estimated using 12 reflection-free points and were not subsequently refined. A refinable overall temperature factor was used to scale individual temperature factors set at single-crystal values. The overall temperature factor acts as an approximate extinction and absorption correction (20). The pattern zero point and unit-cell dimensions were refined. Tetrahedral-side occupancies were refined by constraining the total Ga + Si in each site to unity while the occupancies of each site were varied independent of the other three tetrahedral sites. Occupancy refinements converged rapidly due to the large difference in the X-ray scattering efficiencies of Ga and Si.

#### **Results and Discussion**

The calculated X-ray diffraction patterns for low and high gallium albite (GBF11 and GBF12, respectively) are in good agreement with the observed patterns (e.g., Fig. 1). Residual intensity is largely restricted to the shoulders of high intensity peaks and appears to result from profile functions which do not effectively simulate peak pro-

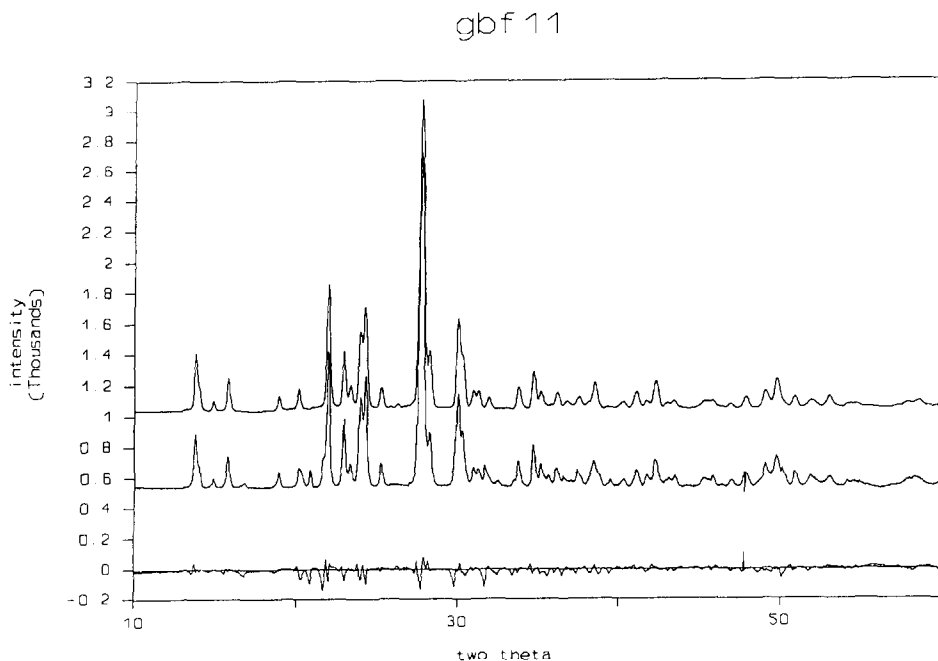


FIG. 1. X-ray powder diffraction patterns for low (ordered) gallium albite (GBF11). (Upper) Calculated from the refined structural parameters; (middle) observed; (lower) residual.

files. Tetrahedral-site occupancies, unit-cell dimensions, and agreement indices are given in Table I. Comparison of the powder diffraction patterns for low, intermediate, and high gallium albite are given in Fig. 1a-c in Burns and Fleet (1).

The present use of the Rietveld technique for structure refinement is primarily limited to the determination of tetrahedral-site Ga/Si occupancies and accurate unit-cell parameters (1). We realized from the outset that the general lack of high-angle data would eliminate the possibility of accurate refinement of temperature factors and coordinate for oxygen atom positions. Nevertheless, the refined atomic coordinates for low and high gallium albite are in fair agreement with the single-crystal values for low and high albite, respectively, when the larger gallium atom is taken into consider-

ation. As expected, the oxygen parameters were the least reliable and were generally unstable toward refinement. However, the large difference in the scattering factors of Ga and Si, which is largest at low angles anyway, made the Rietveld refinements very sensitive to the tetrahedral-site occupancies (1).

The  $^{29}\text{Si}$  MAS NMR spectrum of low gallium albite (GbF11; Fig. 2(a), Table II) consists of three peaks at  $-89.5$ ,  $-96.4$ , and  $-104.2$  ppm, with relative areas of  $0.79:1:0.77$ , which were tentatively assigned to the  $T_2m$ ,  $T_2O$ , and  $T_1m$  sites, respectively, by comparison with the three peaks of equal intensity in the spectrum of (ordered) Amelia albite at  $-92.8$ ,  $-97.1$ , and  $-104.9$  ppm (14).

There is no sign of a fourth peak which could be correlated to the  $T_1O$  site in either

TABLE I  
REFINED UNIT-CELL PARAMETERS,  
TETRAHEDRAL-SITE OCCUPANCIES (Ga), AND  
RIETVELD AGREEMENT INDICES FOR EACH  
REFINEMENT

	GBF11 (low gallium albite)	GBF12 (high gallium albite)
Tetrahedral-site occupancies		
$T_1O$	0.76(3)	0.29(2)
$T_{1m}$	0.11(2)	0.22(2)
$T_2O$	0.02(2)	0.24(2)
$T_{2m}$	0.11(2)	0.26(2)
Unit-cell parameters		
$a$	8.175(1)	8.196(2)
$b$	12.863(2)	12.960(3)
$c$	7.198(1)	7.146(2)
$\alpha$	94.35(1)	93.57(2)
$\beta$	116.471(8)	116.44(1)
$\gamma$	87.312(8)	89.96(2)
Refinement agreement indices <sup>a</sup>		
$R_p$	11.2	12.5
$R_{wp}$	16.3	18.3
$R_{wp}(exp)$	9.3	8.6
$R_B$	10.8	4.3

<sup>a</sup>  $R_p$ , Rietveld profile agreement index;  $R_{wp}$ , Rietveld weighted profile agreement index;  $R_{wp}(exp)$ , expected Rietveld weighted profile agreement index;  $R_B$ , Rietveld Bragg agreement index. Total number of parameters refined: 57.

Note. Errors stated are 1 SD.

the spectrum of low gallium albite or that of Amelia albite. This could be because it is of too low an intensity to be visible above the noise or that it overlaps with one of the other peaks. Si in the  $T_1O$  site would cause disorder in the structure and the intensity from this site could be spread over five different peaks due to differing numbers of Si and Al next nearest neighbors, in which case none of the individual peaks would be intense enough to be separately resolved. Calculations of chemical shift for the  $T_1O$  site for gallium albite with four surrounding Si atoms would give a value of  $-104.9$  ppm (18).

The greatest difference between the spectra of ordered gallium albite and those of Amelia albite is the position of the  $T_{2m}$  peak at  $-89.6$  ppm in gallium albite com-

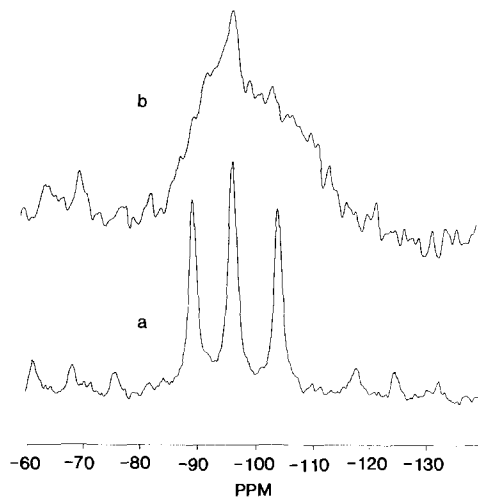


FIG. 2. (a)  $^{29}Si$  MAS NMR spectrum of low (ordered) gallium albite (GBF11). (b)  $^{29}Si$  MAS NMR spectrum of high temperature gallium albite (GBF12).

pared with  $-92.8$  ppm in albite (Table II). There is a slight shift of the other two peaks of  $0.7$  ppm to low field. The effect of Ga/Al replacement would be expected to be the greatest for the  $T_{2m}$  peak as there are two Ga/Al next nearest neighbors rather than the one for  $T_2O$  and  $T_{1m}$ . However, there is a calculated shift of  $0.6$  ppm to high field

TABLE II  
 $^{29}Si$  MAS NMR PARAMETERS FOR LOW (ORDERED)  
GALLIUM ALBITE AND ALBITE

	$T_{2m}$	$T_2O$	$T_{1m}$
Chemical shift (ppm)			
Gallium albite			
Measured	-89.6	-96.4	-104.2
Calculated <sup>a</sup>	-94.4	-97.7	-103.5
Amelia albite			
Measured	-92.8	-97.1	-104.9
Calculated <sup>a</sup>	-93.5	-97.3	-102.8
Si occupancies in gallium albite			
Measured <sup>b</sup>	0.79	1.00	0.77
Calculated <sup>c</sup>	0.89	0.98	0.89

<sup>a</sup> Calculated using the method of Sherriff *et al.* (18).

<sup>b</sup> Measured from relative peak intensities.

<sup>c</sup> Calculated from Rietveld refinement of X-ray data.

with the replacement of one Al by one Ga neighbor and the adjustment of the cation oxygen distance to 1.83 Å (25). This is in the opposite direction to the experimental results but within experimental error (18). From the calculations of chemical shift we would expect that the direct replacement of Al by Ga, without adjustment of bond angles, would have virtually no effect on the  $^{29}\text{Si}$  spectrum, as was found in a study of Ga/Al replacement in aluminosilicate glasses (25). The present shift of all the peaks to low field can be accounted for by a general decrease in the bond angle at the bridging oxygen (Si–O–T) with the replacement of Al by Ga. The reduction in angle at the bridging oxygen must be at least double that for the  $T_2m$  site to account for the 3.2 ppm shift to low field. We were not able to verify this result with the X-ray diffraction studies due to a lack of accuracy in the refined oxygen positional parameters. The single crystal X-ray structure of low gallium albite (6) reveals that, compared with the structure of low albite, the two  $T_2m$ –O–Ga angles do decrease by 4.6° and 2.1°, but  $T_1m$ –O–Ga and  $T_2O$ –O–Ga decrease by 3.6° and 4.9°, respectively.

We did not find any splittings in the peaks of the ordered gallium albite to correspond to the Si/Al spin–spin coupling effect found in Amelia albite by Woessner and Trewella (26). This is not surprising as Ga has two naturally occurring magnetic isotopes  $^{69}\text{Ga}$  and  $^{71}\text{Ga}$  with relative abundances of 60.4 and 39.6%, respectively, and both with spin 3/2. For the  $T_2O$  and  $T_1m$  sites with one neighboring Ga, spin–spin coupling would give two overlapping multiplets of four peaks of equal intensity for each isotope with different  $J$  coupling constants. For the  $T_2m$  site with two Ga neighbors there would be two overlapping quintuplets with a relative intensity of 1 : 2 : 3 : 2 : 1. Woessner and Trewella (26) measured  $^2J_{\text{Al,Si}}$  of 9 Hz. The value of  $^2J$  would be expected to be less for Ga–Si coupling as the Ga–Si distance

would be 0.2 Å longer than that for Si–Al. The slow relaxation rate of the synthetic gallium albite, combined with finite, expensive instrument time, limited the signal/noise ratio that could be obtained. The spectra shown were recorded with 50 Hz of line broadening to reduce the apparent noise but even with less line broadening there was no further resolution of the three peaks.

The spectrum of high gallium albite (GbF12) is a broad envelope of resonances from –85 to –115 ppm with one peak resolved at –96 ppm (Fig. 2(b)). The loss of resolution with increased cation disorder in high gallium albite has also been observed in the spectrum of annealed Amelia albite (14, 27). The range of chemical shifts for high gallium albite is similar to the values of –88 to –111 ppm found for annealed Amelia albite (24) and can be attributed to overlapping peaks from all four tetrahedral sites with next nearest neighbour configurations of 4Ga, 3Ga1Si, 2Ga2Si, 1Ga3Si, and 4Si. We speculate that the apparent resolution of the characteristic  $T_2O$  resonance (at –96 ppm) indicates that proportionately more of the  $T_2O$  sites retain the “low” configuration.

The site occupancies of Si in low gallium albite determined from Rietveld refinement are 0.89, 0.98, and 0.89 for  $T_2m$ ,  $T_2O$ , and  $T_1m$ , respectively. If the  $T_2O$  site is assumed to contain only Si, then the relative peak intensities of the corresponding MAS NMR spectrum (Fig. 2(a)) reveal Si occupancies for  $T_2m$  and  $T_1m$  of 0.77 and 0.79. This agreement in relative site occupancies provides independent proof of the assignment of the –96 ppm resonance to  $T_2O$  in the MAS NMR spectra of albites.

## Conclusion

The ordering of Si in the tetrahedral sites of both high and low structural state gallium albite found by integration of MAS NMR

spectra is in close agreement with the ordering determined by Rietveld structure refinement of X-ray powder diffraction data.

The differences between the peak positions of the  $^{29}\text{Si}$  MAS NMR peaks for low ordered gallium albite and those for Amelia albite are probably due to the differences in angles at the bridging oxygens. This is the first independent assignment of the  $^{29}\text{Si}$  peak at  $-96$  ppm in the spectrum of low albite to the  $T_2O$  site.

### Acknowledgments

We thank B. Sayer of McMaster University for help with instrumentation, J. S. Hartman of Brock University for the use of the MAS probe, the Royal Ontario Museum for loan of the sample of Amelia albite (M 13943), and the reviewer of the manuscript for helpful suggestions. This work was supported by NSERC through an operating grant to MEF, a postdoctoral fellowship to BLS, and a postgraduate scholarship to PCB.

### References

1. P. C. BURNS AND M. E. FLEET, *Phys. Chem. Miner.* **17**, 108 (1990).
2. J. R. GOLDSMITH AND D. M. JENKINS, *Am. Mineral.* **70**, 911 (1985).
3. H. PENTINGHAUS, *Dissertation, Universität Munster* (1970).
4. H. PENTINGHAUS AND H. BAMBAUER, *Neues Jahrb. Mineral. Monatsh.* **94** (1971).
5. D. K. SWANSON AND C. T. PREWITT, "Proceedings, Annual Meeting of the Geological Society of America" (abstract), p. 691, Geological Society of America, Boulder, CO (1984).
6. M. E. FLEET, *Am. Mineral.* **76**, in press (1991).
7. M. E. FLEET, *J. Solid State Chem.*, in press (1991).
8. E. LIPPMAA, M. MÄGI, A. SAMOSAN, G. ENGELHARDT, AND A. -R. GRIMMER, *J. Am. Chem. Soc.* **102**, 4889 (1980).
9. J. B. HIGGINS AND D. E. WOESSNER, *EOS* **63**, 1139 (1982).
10. K. A. SMITH, R. J. KIRKPATRICK, E. OLDFIELD, AND D. M. HENDERSON, *Am. Mineral.* **68**, 1206 (1983).
11. J. V. SMITH, C. S. BLACKWELL, AND G. L. HOVIS, *Nature* **309**, 140 (1984).
12. N. JANES AND E. OLDFIELD, *J. Am. Chem. Soc.* **107**, 6769 (1985).
13. R. J. KIRKPATRICK, R. A. KINSEY, K. A. SMITH, D. M. HENDERSON, AND E. OLDFIELD, *Am. Mineral.* **70**, 106 (1985).
14. B. L. SHERRIFF AND J. S. HARTMAN, *Can. Mineral.* **23**, 203 (1985).
15. B. L. SHERRIFF AND H. D. GRUNDY, *Nature* **332**, 819 (1988).
16. C. A. FYFE, G. C. GOBBI, J. S. HARTMAN, R. E. LENKINSKI, J. H. O'BRIEN, E. R. BEANGE, AND M. A. R. SMITH, *J. Magn. Reson.* **47**, 168 (1982).
17. B. L. SHERRIFF, H. D. GRUNDY, AND J. S. HARTMAN, *Can. Mineral.* **25**, 717 (1987).
18. B. L. SHERRIFF, H. D. GRUNDY, AND J. S. HARTMAN, *Eur. J. Mineral.*, in press. (1991)
19. G. E. HARLOW AND G. E. B. BROWN, JR., *Am. Mineral.* **65**, 986 (1980).
20. M. RAUDSEPP, A. C. TURNOCK, F. C. HAWTHORNE, B. L. SHERRIFF, AND J. S. HARTMAN, *Am. Mineral.* **72**, 580 (1987).
21. R. J. HILL AND C. J. HOWARD, "Australian Atomic Energy Commission Report," No. M112, Australian Atomic Energy Commission, Sutherland, New South Wales, Australia (1986).
22. D. B. WILES AND R. A. YOUNG, *J. Appl. Crystallogr.* **14**, 149 (1981).
23. D. E. APPLEMAN AND H. T. EVANS, "National Technical Information Service Document," PB 216, p. 188, National Technical Information Service (1973).
24. J. V. SMITH, "Feldspar Minerals," Vols. 1 and 2, Springer-Verlag, Berlin (1974).
25. B. L. SHERRIFF AND M. E. FLEET, *J. Geophys. Res.* **95**, 15727 (1990).
26. D. E. WOESSNER AND J. C. TREWELLA, *J. Magn. Reson.* **59**, 352 (1984).
27. W-H. YANG, R. J. KIRKPATRICK, AND D. M. HENDERSON, *Am. Mineral.* **71**, 712 (1986).